AD-203 077

UNCLASSIFIED
SECURITY CLASSIFICATION OF THIS PAGE

2

REPORT DOCUMENTATION PAGE

Form Approved
OMB No. 0704-0188

1a. REPORT SECURITY CLASSIFICATION: UNCLASSIFIED	1b. RESTRICTIVE MARKINGS
2a. SECURITY CLASSIFICATION AUTHORITY	3. DISTRIBUTION/AVAILABILITY OF REPORT: Approved for public release, distribution unlimited
2b. DECLASSIFICATION/DOWNGRADING SCHEDULE	
4. PERFORMING ORGANIZATION REPORT NUMBER(S): TELAC Report 88-11	5. MONITORING ORGANIZATION REPORT NUMBER(S): AFOSR-TR- 88-1289
6a. NAME OF PERFORMING ORGANIZATION: Technology Laboratory for Advanced Composites, Massachusetts Institute of Technology; 6b. OFFICE SYMBOL (If applicable)	7a. NAME OF MONITORING ORGANIZATION: AFOSR
6c. ADDRESS (City, State, and ZIP Code): M.I.T.; Room 33-309, 77 Massachusetts Avenue, Cambridge, Mass. 02139	7b. ADDRESS (City, State, and ZIP Code): same as 8c.
8a. NAME OF FUNDING/SPONSORING ORGANIZATION: AFOSR; 8b. OFFICE SYMBOL (If applicable): NA	9. PROCUREMENT INSTRUMENT IDENTIFICATION NUMBER: F49620-86-C-0046
8c. ADDRESS (City, State, and ZIP Code): Bolling Air Force Base, Washington, DC 20332	10. SOURCE OF FUNDING NUMBERS: PROGRAM ELEMENT NO. 61102F; PROJECT NO. 2302; TASK NO. B1; WORK UNIT ACCESSION NO.

DTIC ELECTE DEC 16 1988 S E

11. TITLE (Include Security Classification)

Stall Flutter of Graphite/Epoxy Wings with Bending-Torsion Coupling

12. PERSONAL AUTHOR(S)

Peter Dunn & John Dugundji

13a. TYPE OF REPORT	13b. TIME COVERED	14. DATE OF REPORT (Year, Month, Day)	15. PAGE COUNT
Annual Technical Report	FROM 7/1/87 TO 6/30/88	1988 October 25	23

16. SUPPLEMENTARY NOTATION

17. COSATI CODES			18. SUBJECT TERMS (Continue on reverse if necessary and identify by block number)
FIELD	GROUP	SUB-GROUP	

19. ABSTRACT (Continue on reverse if necessary and identify by block number)

An analytical and experimental investigation is made of the non-linear, large amplitude, high angle of attack, stall flutter behavior of cantilevered graphite/epoxy wings. Ten six-ply graphite/epoxy wings with a wide range of bending-torsion characteristics were constructed and styrofoam fairings epoxied to these to form NACA-0012 airfoil shapes. Wind tunnel tests on these cantilevered wings revealed torsional and bending stall flutter limit cycles, depending on the layup. Reasonable agreement with steady, non-linear theory and with unsteady, linear theory was found. Fourier analysis applied to the ONERA 2-dimensional, non-linear, unsteady, aerodynamic model shows reasonable agreement with 2-dimensional experiments on aerodynamic force and moment coefficients. A 3-dimensional, non-linear, unsteady, aeroelastic analysis with a Newton-Raphson solver applied to the harmonic balance method is developed to attempt to predict the non-linear, stall flutter observed in the experiment. Final results of this analysis are currently being completed and will appear shortly in a forthcoming report.

20. DISTRIBUTION/AVAILABILITY OF ABSTRACT	21. ABSTRACT SECURITY CLASSIFICATION
☑ UNCLASSIFIED/UNLIMITED ☑ SAME AS RPT. ☐ DTIC USERS	UNCLASSIFIED
22a. NAME OF RESPONSIBLE INDIVIDUAL: Dr. Anthony K. Amos	22b. TELEPHONE (Include Area Code): (202) 767-0468; 22c. OFFICE SYMBOL: NA

DD Form 1473, JUN 86 — Previous editions are obsolete. — SECURITY CLASSIFICATION OF THIS PAGE

UNCLASSIFIED

STALL FLUTTER OF GRAPHITE/EPOXY WINGS WITH BENDING-TORSION COUPLING

Peter Dunn

John Dugundji

Technology Laboratory for Advanced Composites

Department of Aeronautics and Astronautics

Massachusetts Institute of Technology

Cambridge, Massachusetts 02139

October 1988

Annual Technical Report for Period: 1 JULY 87 - 30 JUNE 88

AFOSR Contract No.: F49620-86-C-0066

ABSTRACT

An analytical and experimental investigation is made of the non-linear, large amplitude, high angle of attack, stall flutter behavior of cantilevered graphite/epoxy wings. Ten six-ply graphite/epoxy wings with a wide range of bending-torsion characteristics were constructed and styrofoam fairings epoxied to these to form NACA-0012 airfoil shapes. Wind tunnel tests on these cantilevered wings revealed torsional and bending stall flutter limit cycles, depending on the layup. Reasonable agreement with steady, non-linear theory and with unsteady, linear theory was found. Fourier analysis applied to the ONERA 2-dimensional, non-linear, unsteady, aerodynamic model shows reasonable agreement with 2-dimensional experiments on aerodynamic force and moment coefficients. A 3-dimensional, non-linear, unsteady, aeroelastic analysis with a Newton-Raphson solver applied to the harmonic balance method is developed to attempt to predict the non-linear, stall flutter observed in the experiment. Final results of this analysis are currently being completed, and will appear shortly in a forthcoming report.

FOREWORD

This report describes work done at the Technology Laboratory for Advanced Composites (TELAC) at the Massachusetts Institute of Technology for the Air Force under Contract No. F49620-86-C-0066. Dr. Anthony K. Amos was the contract monitor.

The work reported herein was performed during the period 1 July 1987 through 30 June 1988. The work represents the efforts of one graduate student, Peter Dunn, and an undergraduate student, Chakko Kovoor, under the direction of Principal Investigator, John Dugundji, and the supporting laboratory staff.

1. INTRODUCTION

The present research is part of a continuing investigation into the aeroelastic flutter and divergence behavior of forward-swept, graphite/epoxy composite wing aircraft. The specific objectives of the current investigation are to investigate experimentally and analytically, the roles of non-linear structures and non-linear aerodynamics in large amplitude, high angle-of-attack stall flutter of aeroelastically tailored wings.

In previous investigations at M.I.T., the aeroelastic flutter and divergence behavior of cantilevered, unswept and swept, graphite/epoxy wings was investigated in a small, low-speed wind tunnel. The wings were six-ply, graphite/epoxy plates with strong bending-twisting coupling. Experiments were conducted to determine the flutter boundaries of these wings both at low and high angles of attack, stall flutter often being observed in the latter. Steady, non-linear aerodynamics correlated well before the onset of flutter, and the divergence and flutter results at low angles of attack correlated well with linear, unsteady theory, indicating some beneficial effects of ply orientation in aeroelastic behavior (References 1, 2, and 3). But no non-linear, unsteady analyses were attempted for the higher angles of attack.

Recently, Tran and Petot (Reference 4) and Dat and Tran (Reference 5) of *Office National d'Etudes et de Recherches Aerospatiales* have developed a semi-empirical, unsteady, non-linear model (called the ONERA model) for determining the

2-dimensional aerodynamic forces on an airfoil oscillating in pitch only which experiences dynamic stall. This model incorporates a single lag term operating on the linear part of the airfoil's static lift curve, thus analogous to the Theodorsen function for linear, flat-plate theory, and a two lag term operating on the non-linear (i.e. stalling) part of the airfoil's static lift curve. The semi-empirical coefficients of the non-linear aerodynamics for the ONERA model were determined for various airfoils and the model applied as a comparison against experiment by Dat, Tran, and Petot. Further analysis of the model was done by Peters (Reference 6) to differentiate the roles of angle of attack due to pitching (θ) and angle of attack due to plunging ($\dot{h}/U$), and by Petot and Dat (Reference 7) to reformulate the equations so that they reduce to the Theodorsen function in the case of a flat plate in the linear domain. Additionally, Petot and Loiseau (Reference 8) have contributed corrections to the ONERA model for low Reynold's number flows, in the regime of the current investigation. Generally, however, little work has been done in implementing the ONERA model in a non-linear, aeroelastic flutter analysis. The present research plans to use the non-linear ONERA model to help analytically explain some of the stall flutter behavior observed earlier in the experimental tests.

2. PRESENT WORK

The present investigation deals with the effects of large amplitude deflections and non-linear, unsteady, stalled aerodynamics on the aeroelastic behavior of aeroelastically tailored wings. Six-ply, graphite/epoxy wings with a wide range of bending-torsion characteristics were previously constructed with styrofoam fairings epoxied to these to form NACA-0012 airfoil shapes. These wings were mounted vertically with cantilevered root conditions inside the M.I.T. Department of Aeronautics and Astronautics 5 x 7 ft (1.5 m x 3 m) low speed acoustic wind tunnel, and tested to velocities of 30 m/s. Figures 1 and 2 show the wing construction and the typical setup in the wind tunnel. Ten different ply layups were tested, namely $[0_2/90]_s$, $[90/0_2]_s$, $[+15_2/0]_s$, $[-15_2/0]_s$, $[+30_2/0]_s$, $[-30_2/0]_s$, $[\pm 15/0]_s$, $[\mp 15/0]_s$, $[\pm 30/0]_s$, and $[\mp 30/0]_s$. These wing surfaces include some of those used in previous cantilever tests (References 1, 2, and 3), so that the reproducibility of those previous tests could be verified.

Static bending and free vibration bench tests were conducted to verify the mass, stiffness, and bending-torsion properties of the wings. The wind tunnel tests included divergence and limit cycle flutter testing at both low and high speeds, with root angle of attack varying from zero to more than twice the static stall angle. Data was recorded for wing bending and wing torsion moments on floppy disk via a Nicolet digital oscilloscope using strain gauges located

near the roots of the wings. Video movies were also taken to record tip deflection and tip twist. The experimental data from these test was processed and analyzed during the current reporting period. A typical example of some of the observed flutter boundaries is indicated in Figure 3.

An analytical investigation was also made concurrently with the experimental tests. This involved a 5-degree of freedom Rayleigh-Ritz flutter analysis using the 5 modes, $q_i(t)$, similar to those of References 2 and 3 (i.e. 1st and 2nd wing bending, 1st and 2nd wing torsion, and 1st chordwise bending). The wing torsion modes, which previously only reflected the root warping effects on the natural frequencies of the wings, were altered to also reflect the root warping effects on the tip deflection, and were also modified to include a simple, non-linear, cubic stiffening effect.

The aerodynamic analysis employed a 2-dimensional, unsteady, non-linear strip theory with spanwise correction for finite span effects. The aerodynamic forces, namely the lift coefficient C_L, the moment coefficient C_M, and the drag coefficient C_D, were taken from the ONERA model (Reference 7) in the form:

$$C_z = C_{z1} + C_{z2}$$

$$C_{z1} = s_z \overset{*}{\alpha} + k_{vz} \overset{**}{\theta} + C_{\gamma_1}$$

$$\overset{*}{C}_{\gamma_1} + \lambda_z C_{\gamma_1} = \lambda_z [a_{oz}\alpha + \sigma_z \overset{*}{\theta}] + \alpha_z [a_{oz} \overset{*}{\alpha} + \sigma_z \overset{**}{\theta}]$$

$$\overset{**}{C}_{z2} + 2dw\overset{*}{C}_{z2} + w^2(1+d^2)C_{z2} =$$

$$= -w^2(1+d^2)\left[\Delta C_z\Big|_\alpha + e\frac{\partial \Delta C_z}{\partial \tau}\Big|_\alpha\right]$$

where,

$$\alpha = \theta - \overset{*}{\bar{h}}$$

$$(^*) \equiv \frac{\partial(\ )}{\partial \tau} \quad ; \quad \tau \equiv \frac{Ut}{b}$$

and,

θ = instantaneous angle of attack

h = instantaneous deflection of 1/4-chord

$\bar{h} \equiv \frac{h}{b}$ = non-dimensional deflection

α = effective angle of attack

and where a_{oz} is the slope of the linear part of the static force curve, ΔC_z is the non-linear deviation from the extended linear lift curve, and s_z, k_{vz}, σ_z, λ_z, δ_z, d, w, and e are previously determined, semi-empirical lag coefficients. In the above formulation, C_{z1} represents the usual linear force, while C_{z2} represents the additional non-linear stalling contribution. The C_{γ_1} term is the circulatory part of the linear lift force. Fourier analysis is used to extract the low harmonic components (1st and 2nd harmonics) from the non-linear forcing terms of these differential equations, by assuming simple harmonic motion for $\bar{h}(t)$ and $\theta(t)$.

A harmonic balance method is then used to set up the coupled, non-linear equations of motion, which incorporate the force coefficients from the above equations. First, the components of the force coefficients are determined assuming

a sinusoidally varying input for the angle of attack and the 1/4-chord deflection,

$$\theta(\tau) = \theta_o + \theta_s \sin(k\tau) + \theta_c \cos(k\tau)$$

$$\bar{h}(\tau) = \bar{h}_o + \bar{h}_s \sin(k\tau) + \bar{h}_c \cos(k\tau)$$

The circulatory part of the linear contribution to the 2-dimensional aerodynamics is given by,

$$C\gamma_{1o}(x) = a_{oz}\theta_o(x)$$

$$C\gamma_{1s}(x) = F(k)L_s(x) - G(k)L_c(x)$$

$$C\gamma_{1c}(x) = G(k)L_s(x) + F(k)L_c(x)$$

where, in the present analysis, the F and G functions are the resulting single lag approximations to the Theodorsen function, $C(k) = F(k)+iG(k)$, namely,

$$F(k) = \frac{\lambda_z^2 + \alpha_z k^2}{\lambda_z^2 + k^2}$$

$$G(k) = -\frac{\lambda_z k(1-\alpha_z)}{\lambda_z^2 + k^2}$$

and where the intermediate variables, $L_s(x)$ and $L_c(x)$, are determined from θ_o, θ_s, θ_c and $\bar{h}_o$, $\bar{h}_s$, $\bar{h}_c$,

$$L_s(x) = a_{oz}\left[\theta_s(x) + k\bar{h}_c(x)\right] - \sigma_z k\theta_c(x)$$

$$L_c(x) = a_{oz}\left[\theta_c(x) - k\bar{h}_s(x)\right] + \sigma_z k\theta_s(x)$$

The complete linear contribution C_{z1o}, C_{z1s}, C_{z1c} is then found by adding in the average, sine, and cosine components of the non-circulatory terms $s_z\overset{*}{\alpha}$ and $k_{vz}\overset{**}{\theta}$.

Similarly, the components of the non-linear contribution, C_{z2o}, C_{z2s}, and C_{z2c}, are determined from the ΔC_{zo}, ΔC_{zs}, and ΔC_{zc} components of the non-linear deviation, $\Delta C_z(\tau)$, as,

$$C_{z20}(x) = -\Delta C_{z0}(x)$$

$$C_{z2s}(x) = \frac{K_1K_3 + K_2K_4}{K_1^2 + K_2^2}$$

$$C_{z2c}(x) = \frac{K_1K_4 - K_2K_3}{K_1^2 + K_2^2}$$

where the intermediate variables, K_1 to K_4, are given by,

$$K_1 = 1 + d^2 - \left(\frac{k}{w}\right)^2$$

$$K_2 = 2d\frac{k}{w}$$

$$K_3 = -(1+d^2)\left[\Delta C_{zs}(x) - ek\Delta C_{zc}(x)\right]$$

$$K_4 = -(1+d^2)\left[\Delta C_{zc}(x) + ek\Delta C_{zs}(x)\right]$$

The equations of motion for the bending-torsion flutter of the wings were set up in harmonic balance form using the 5 modes, $q_i(\tau)$, mentioned earlier, and considering only the constant part and lowest harmonic of each coordinate,

$$q_i(\tau) = q_{io} + q_{is}\sin(k\tau) + q_{ic}\cos(k\tau)$$

The resulting form of the equations of motion is given by the 3n coupled equations:

$$\begin{bmatrix} [K] & 0 & 0 \\ 0 & -\omega^2[M]+[K] & 0 \\ 0 & 0 & -\omega^2[M]+[K] \end{bmatrix} \begin{bmatrix} \{q_o\} \\ \{q_s\} \\ \{q_c\} \end{bmatrix} = \begin{bmatrix} \{Q_o\} \\ \{Q_s\} \\ \{Q_c\} \end{bmatrix}$$

where $\{q_o\}$, $\{q_s\}$, and $\{q_c\}$ are vectors representing the harmonic components of the five coordinates, $q_i(\tau)$, and [M] and [K] are the appropriate mass and stiffness terms. The $\{Q_o\}$, $\{Q_s\}$, and $\{Q_c\}$ are the corresponding harmonic modal forces obtained by integrating the non-linear, 2-dimensional air forces, C_z, over the span of the wing, after having expressed the angle of attack θ and deflection $\bar{h}$ in terms of the coordinates $q_i(\tau)$.

The non-linear equations of motion are then solved using a Newton-Raphson scheme similar to that used by Kuo, Morino, and Dugundji (Reference 9) for a related, non-linear panel flutter problem. The 3n non-linear equations are expressed in the form $\mathbf{f}(\mathbf{x})=0$, and the sine component of one mode $q_i(\tau)$ is set to some small constant to set the amplitude level, while its cosine component is set to zero, since the flutter limit cycle oscillations can start at an arbitrary phase. The Newton-Raphson scheme then uses the 3n equations of motion to solve for the remaining 3n-2 modal component amplitudes, and for the frequency of oscillation, k, and flutter velocity, V. Because the sinusoidal component of one mode shape has

already been set to a non-zero value, the Newton-Raphson scheme does not converge to the trivial steady solution. The Newton-Raphson scheme takes an initial guess of the state vector $\mathbf{x}$ and drives the residual of the equations $\mathbf{f}(\mathbf{x})$ toward zero by inverting the Jacobian matrix (derivative matrix) and obtaining a correction $\Delta\mathbf{x}$ to the current guess. The process is repeated until the correction $\Delta\mathbf{x}$ becomes negligible.

$$\Delta\mathbf{x}^{(n)} = -\left[\frac{d\mathbf{f}}{d\mathbf{x}}\right]_n^{-1} \mathbf{f}(\mathbf{x}^{(n)}) \quad ; \quad \mathbf{x}^{(n+1)} = \mathbf{x}^{(n)} + \Delta\mathbf{x}^{(n)}$$

This Newton-Raphson, harmonic balance scheme has already been used to obtain the linear flutter solution, and is currently being applied to obtain the corresponding non-linear flutter solution by working up from the linear solution.

Comparison of experimental flutter boundaries with those obtained from previous experiments indicates good agreement, thus demonstrating good reproducibility of the experiments. The static tip deflection and static tip twist for all the wings were reasonably predicted by the steady, non-linear analysis, as indicated in Figures 4 and 5. The unsteady, linear analysis reasonably predicted the experimental flutter boundaries at low angles of attack. The Fourier decomposition used here for the ONERA model reasonably predicted the 2-dimensional, unsteady experiments of McAlister, Pucci, McCroskey, and Carr (Reference 10), as indicated in Figures 6 and 7. The unsteady, non-linear analysis described here is almost completed. The trends in the experimental data indi-

cate that the average unsteady tip deflection and tip twist depart from the predicted static tip deflection and static tip twist once flutter oscillations begin, as indicated in Figures 4 and 5. These results appear to indicate a non-linear coupling between the non-linear, static divergence problem and the non-linear, stall flutter problem.

Final results of the present investigation are currently being completed and will appear in a M.S. thesis by the first author, in the near future. This forthcoming thesis will present the final results of the unsteady, non-linear analysis and will compare those results in detail with the experimental data.

3. ACCOMPLISHMENTS

An experimental and analytical investigation is being made of the linear and non-linear aeroelastic flutter and divergence behavior of graphite/epoxy cantilevered wings. Experimental wind tunnel flutter data was obtained at low and high angles of attack in a low speed wind tunnel, for cantilevered wings with NACA-0012 airfoil shapes, and with a wide range of bending-torsion characteristics.

Stall flutter limit cycles were observed experimentally with strain gauge and video data taken. Torsional and bending flutter were observed depending on layup. These experiments confirm earlier linear analytical findings and indicate a non-linear coupling of oscillatory and non-oscillatory aerodynamics resulting in deviation from the predicted steady

analysis. An analytic method has been developed to incorporate non-linear aerodynamics into the aeroelastic model, and to solve the resulting coupled, non-linear flutter problem. In the current case, the non-linear flutter problem couples with the non-linear, stalled divergence problem, and the two problems must be solved together.

The present investigation enlarges the experimental base for aeroelastic tailoring with composites, extending the data base into the range of non-linear, high angle-of-attack flutter. Along with the corresponding theoretical analyses, these should provide insight into the actual aeroelastic behavior of composite wings experiencing dynamic stall.

REFERENCES

1. Hollowell, S.J., and Dugundji, J., "Aeroelastic Flutter and Divergence of Stiffness Coupled, Graphite/Epoxy Cantilevered Plates," Journal of Aircraft, Vol. 21, No. 1, January 1964, pp. 69-76.

2. Selby, H.P., "Aeroelastic Flutter and Divergence of Rectangular Wings with Bending-Torsion Coupling," Masters Thesis, M.I.T., January 1982.

3. Landsberger, B., and Dugundji, J., "Experimental Aeroelastic Behavior of Unswept and Forward Swept Graphite/Epoxy Wings," Journal of Aircraft, Vol. 22, No. 8, August 1985, pp. 679-686.

4. Tran, C.T., and Petot, D., "Semi-Empirical Model for the Dynamic Stall of Airfoils in View of Application to the Calculation of Responses of a Helicopter in Forward Flight," Vertica, Vol. 5, No. 1, 1981, pp. 35-53.

5. Dat, D., and Tran, C.T., "Investigation of the Stall Flutter of an Airfoil with a Semi-Empirical Model of 2-D Flow," Vertica, Vol. 7, No. 2, 1983, pp. 73-86.

6. Peters, D.A., "Toward a Unified Lift Model for Use in Rotor Blade Stability Analyses," Journal of the American Helicopter Society, July 1985, pp. 32-42.

7. Petot, D., and Dat, R., "Unsteady Aerodynamic Loads on an Oscillating Airfoil with Unsteady Stall," 2nd Workshop on Dynamics and Aeroelastic Stability Modeling of Rotorcraft Systems, Florida Atlantic University, Boca Raton, Florida, USA, November, 1987.

8. Petot, D., and Loiseau, H., "Successive Smoothing Algorithm for Constructing the Semi-Empirical Model Developed at ONERA to Predict Unsteady Aerodynamic Forces," NASA TM-76681, March, 1982.

9. Kuo, C.E., Morino, L., and Dugundji, J., "Perturbation and Harmonic Balance Methods for Nonlinear Panel Flutter," AIAA Journal, Vol. 10, No. 11, November, 1972.

10. McAlister, K.W., Pucci, S.L., McCroskey, W.J., and Carr, L.W., "An Experimental Study of Dynamic Stall on Advanced Airfoil Sections Volume 2: Pressure and Force Data," NASA TM-84245, September, 1982.

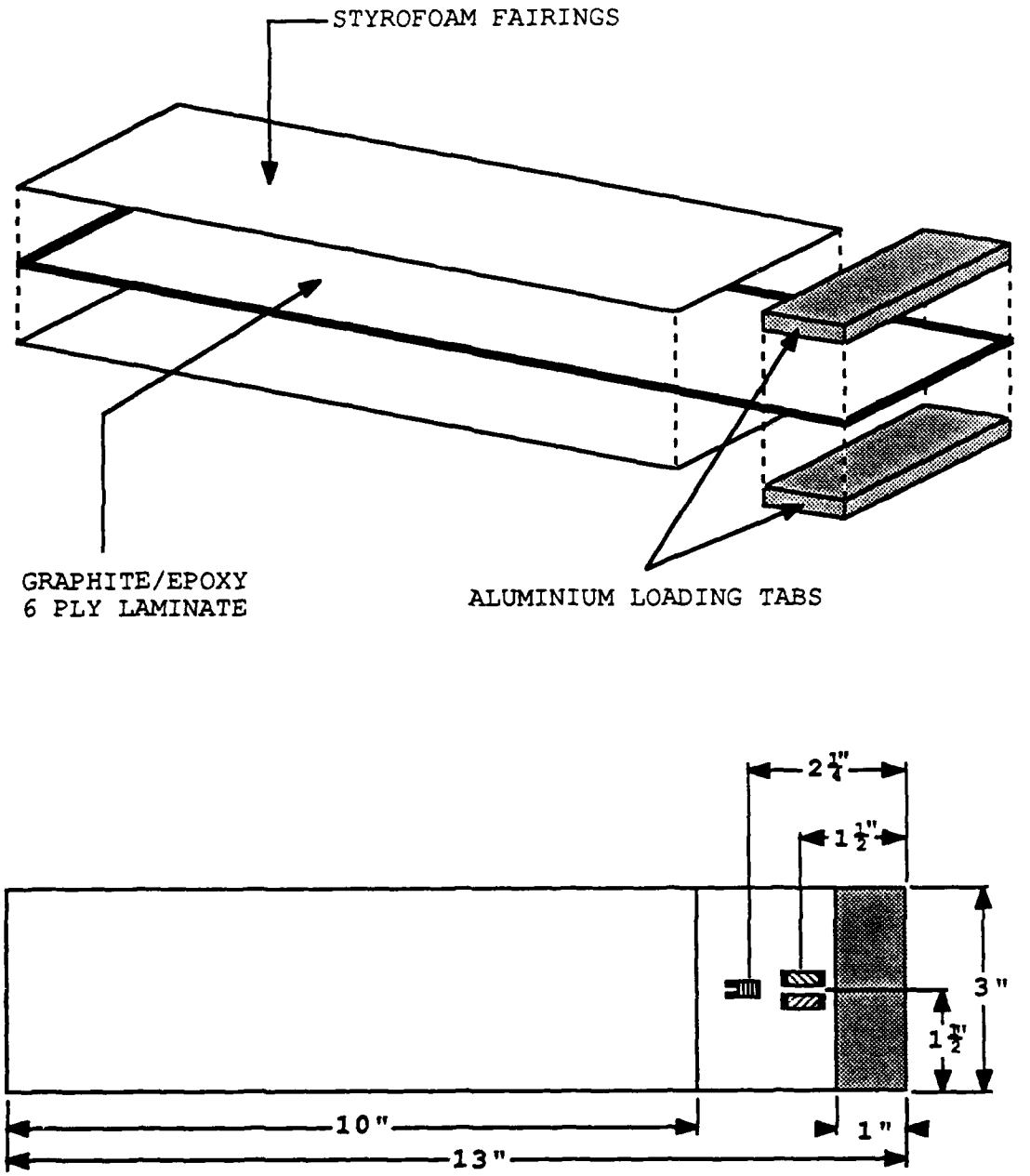

Figure 1 - Wing construction and dimensions

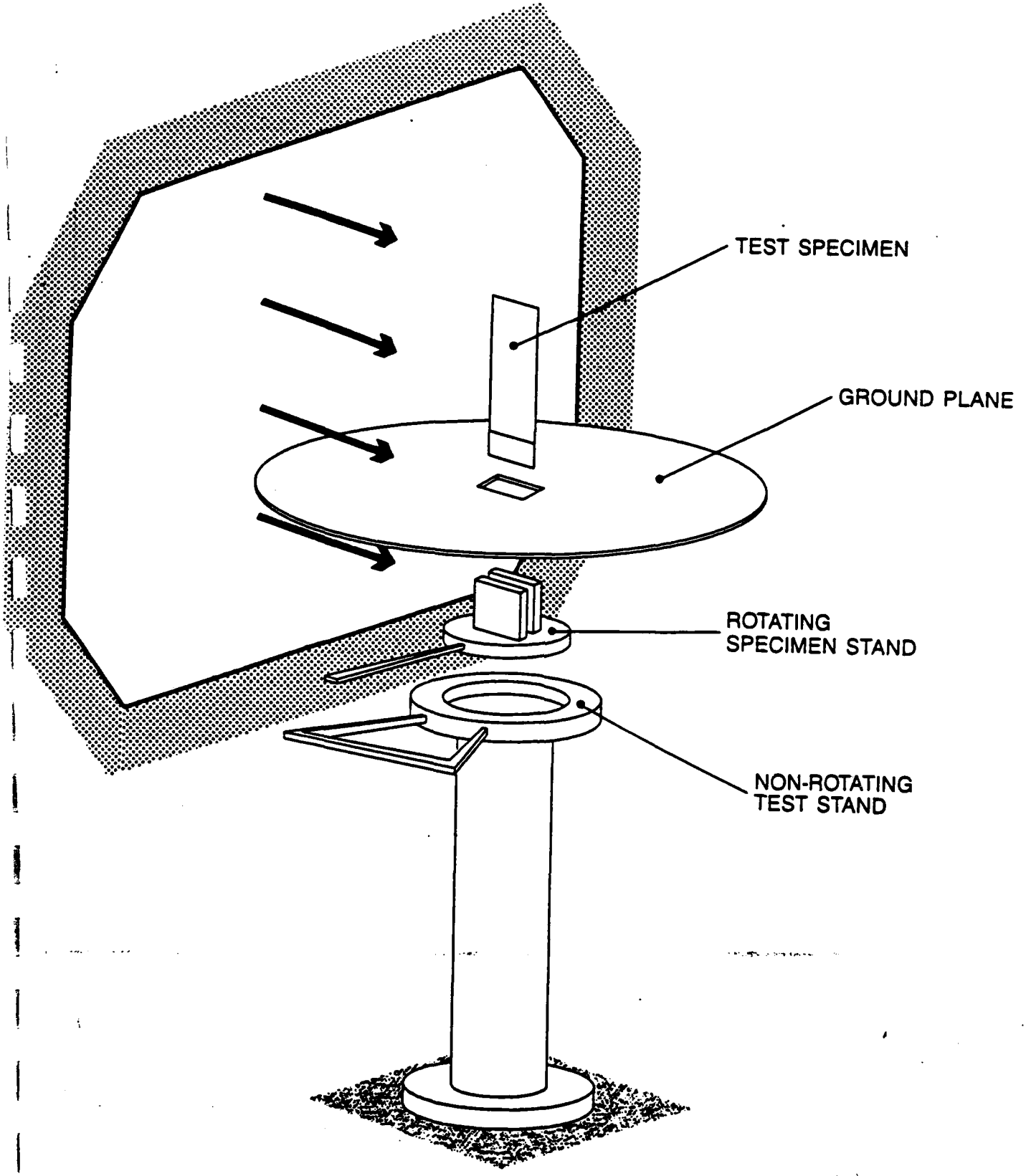

Figure 2 - Experimental setup in wind tunnel

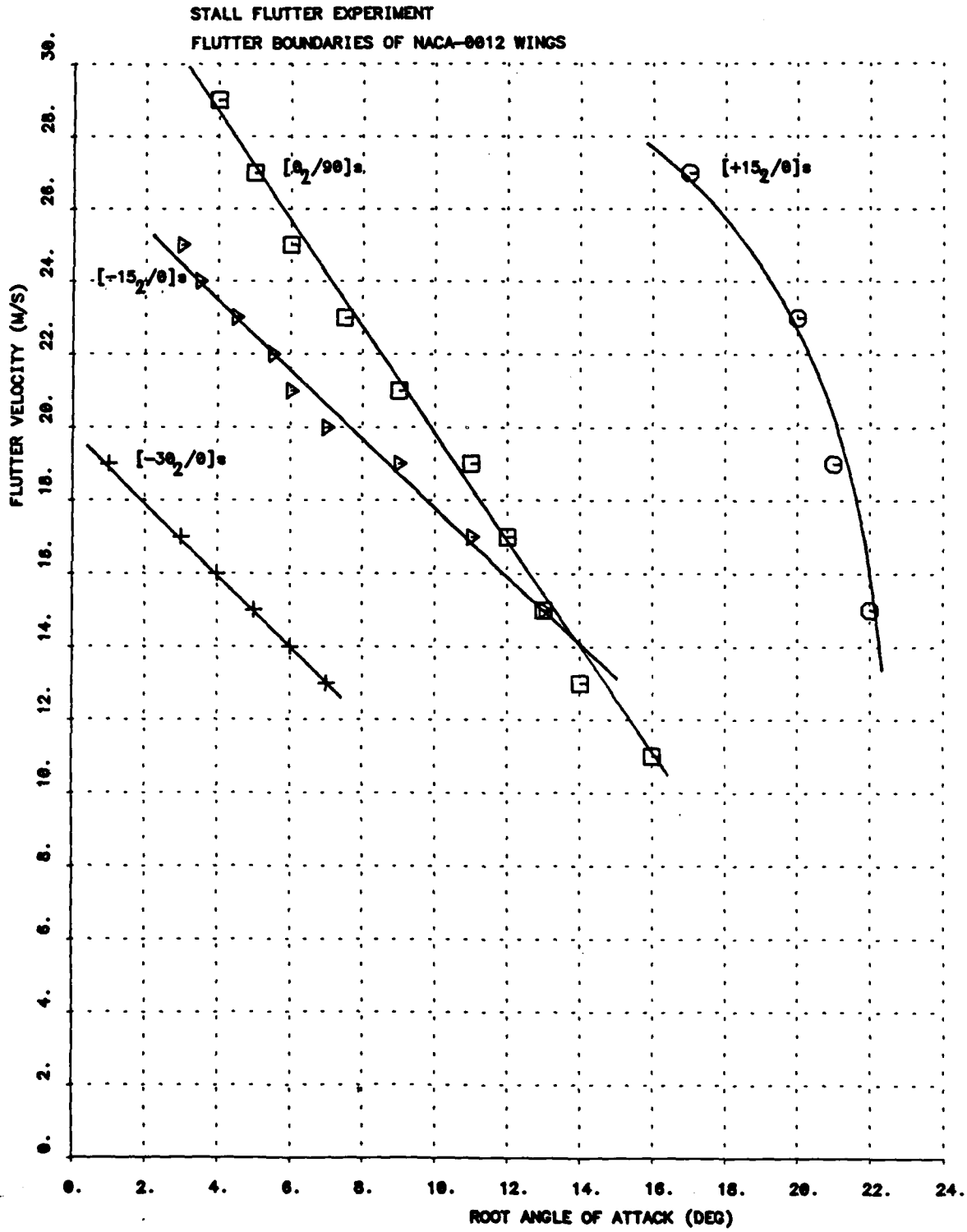

Figure 3 - Experimental flutter boundaries for $[0_2/90]_s$, $[+15_2/0]_s$, $[-15_2/0]_s$, and $[-30_2/0]_s$ NACA-0012 wings

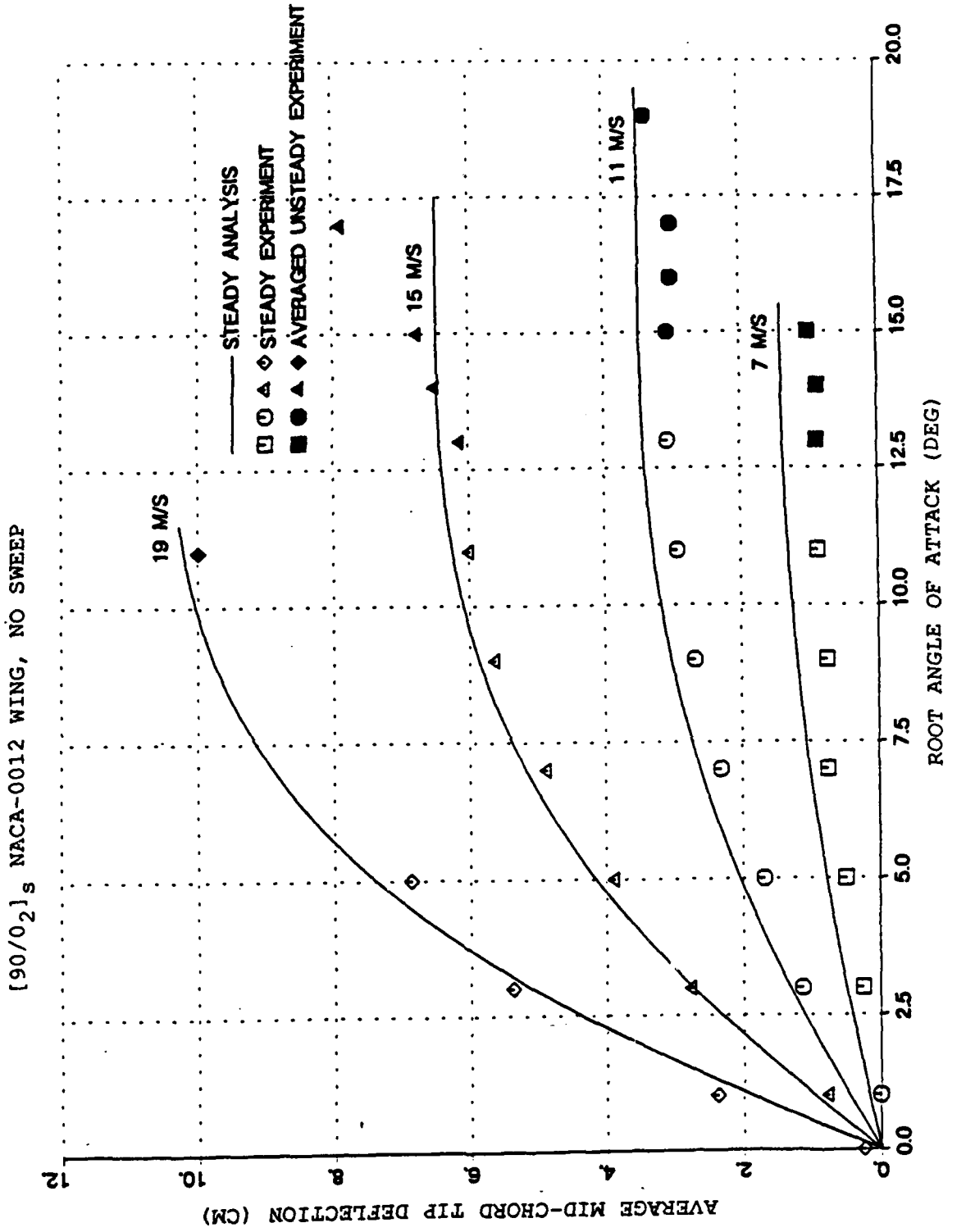

Figure 4 - Average tip deflection vs. root angle of attack

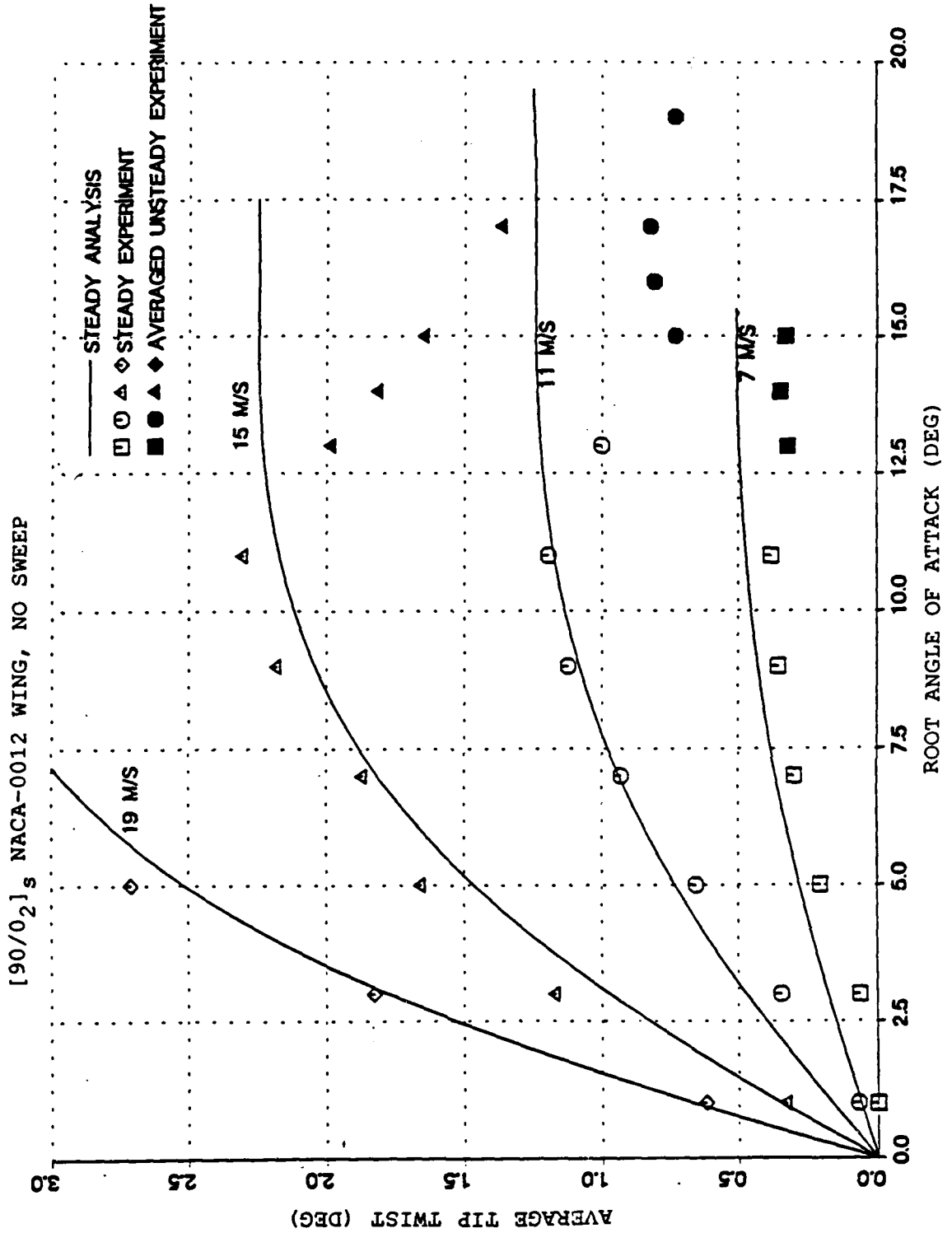

Figure 5 - Average tip twist vs. root angle of attack

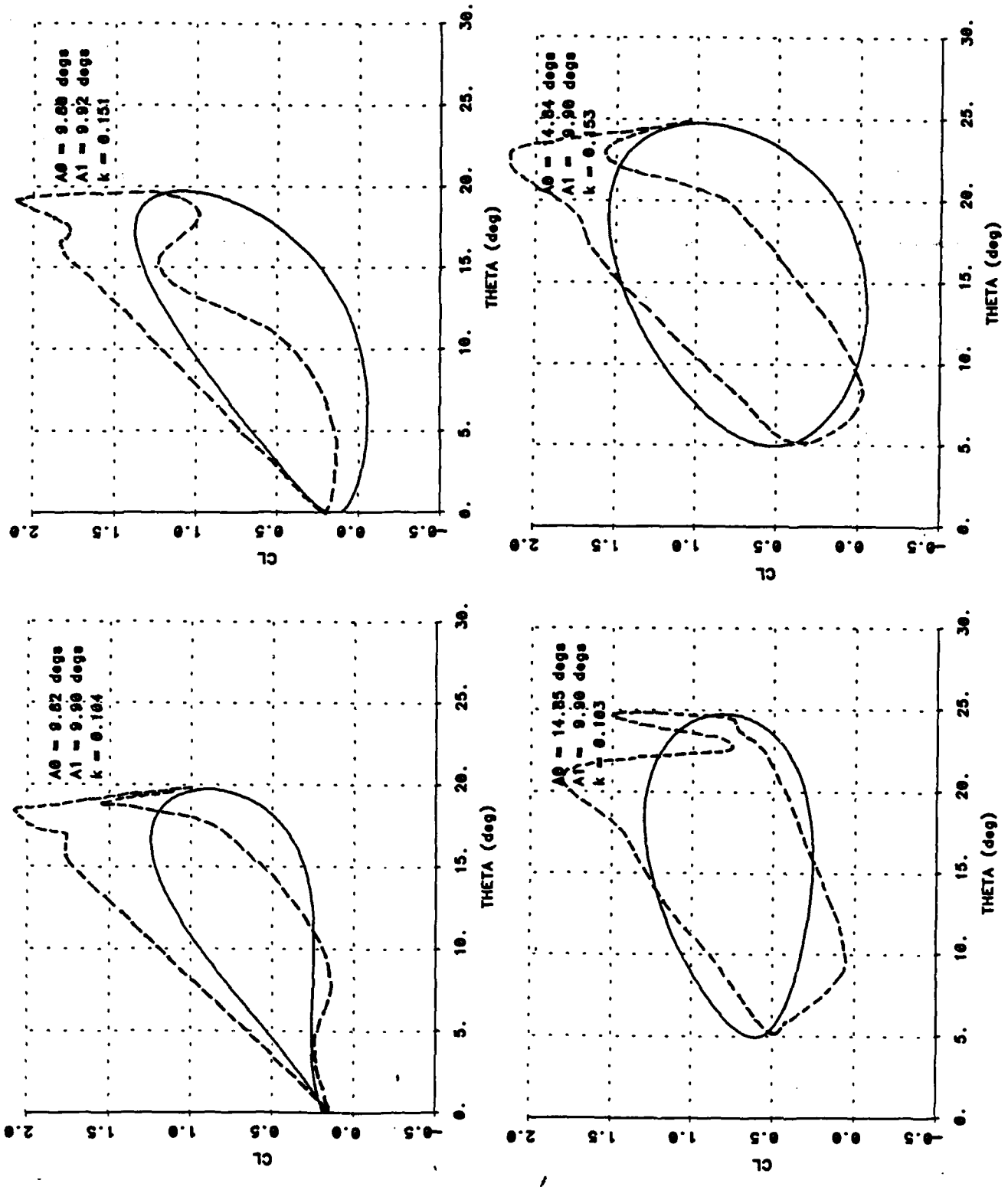

Figure 6 - Hysteresis loops for 2-dimensional lift coefficient versus angle of attack, NACA-0012 airfoil, Re = 0.49 E6 (corrected for wind tunnel effects), compared against McAlister, Pucci, McCroskey, and Carr (Reference 10). —— Analysis --- Experiment

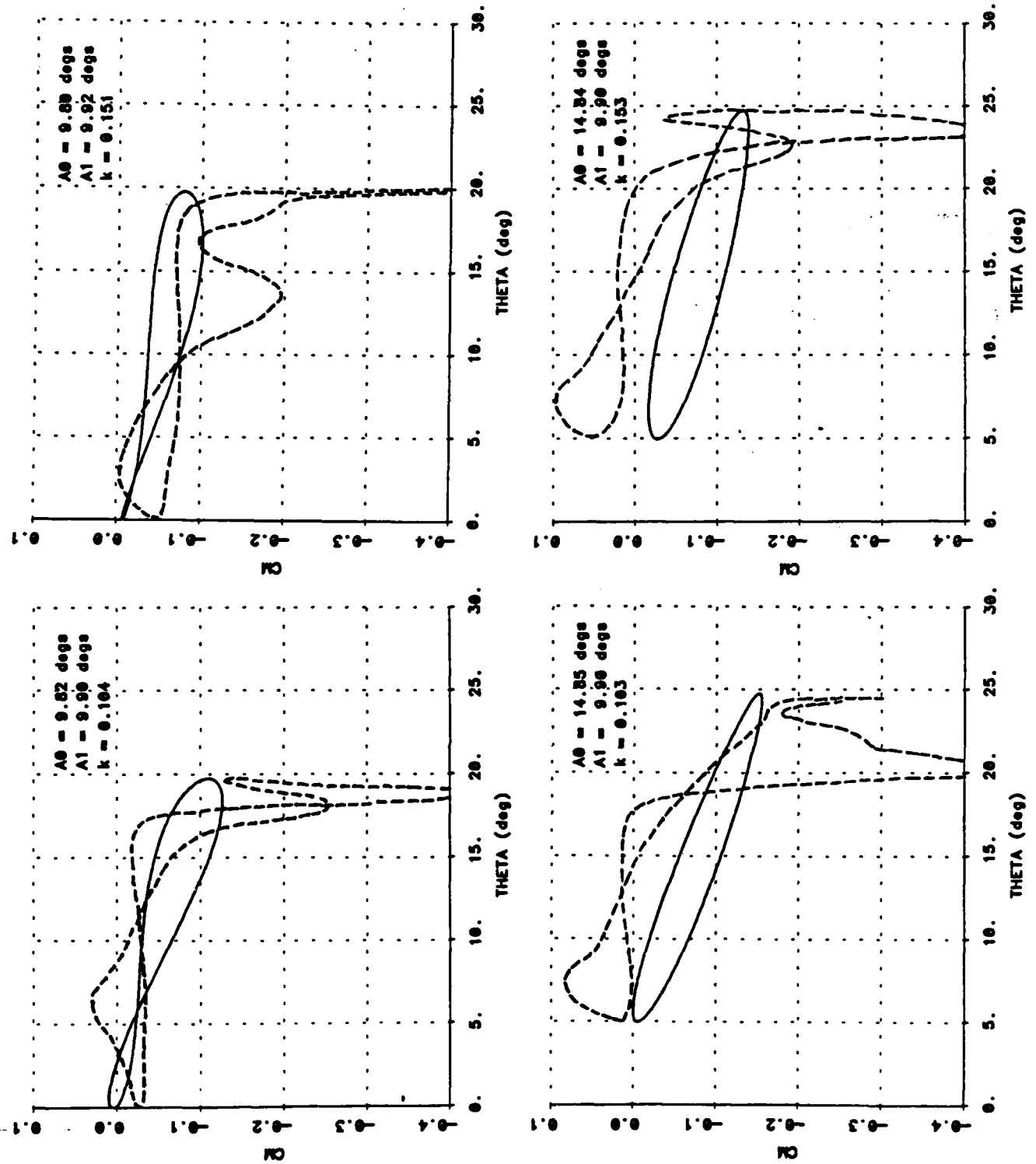

Figure 7 - Hysteresis loops for 2-dimensional moment coefficient versus angle of attack, NACA-0012 airfoil, Re = 0.49 E6 (corrected for wind tunnel effects), compared against McAlister, Pucci, McCroskey, and Carr (Reference 10). —— Analysis --- Experiment